

## Supporting Information

### **A thermolysis approach to simultaneously achieve crystal phase- and shape-control of ternary M-Fe-O metal oxide nanoparticles**

*Chih-Chia Huang, Chich-Neng Chang and Chen-Sheng Yeh\**

*Department of Chemistry and Center for Micro/Nano Science and Technology,*

*National Cheng Kung University, Tainan 701*

*E-mail: [csyeh@mail.ncku.edu.tw](mailto:csyeh@mail.ncku.edu.tw)*

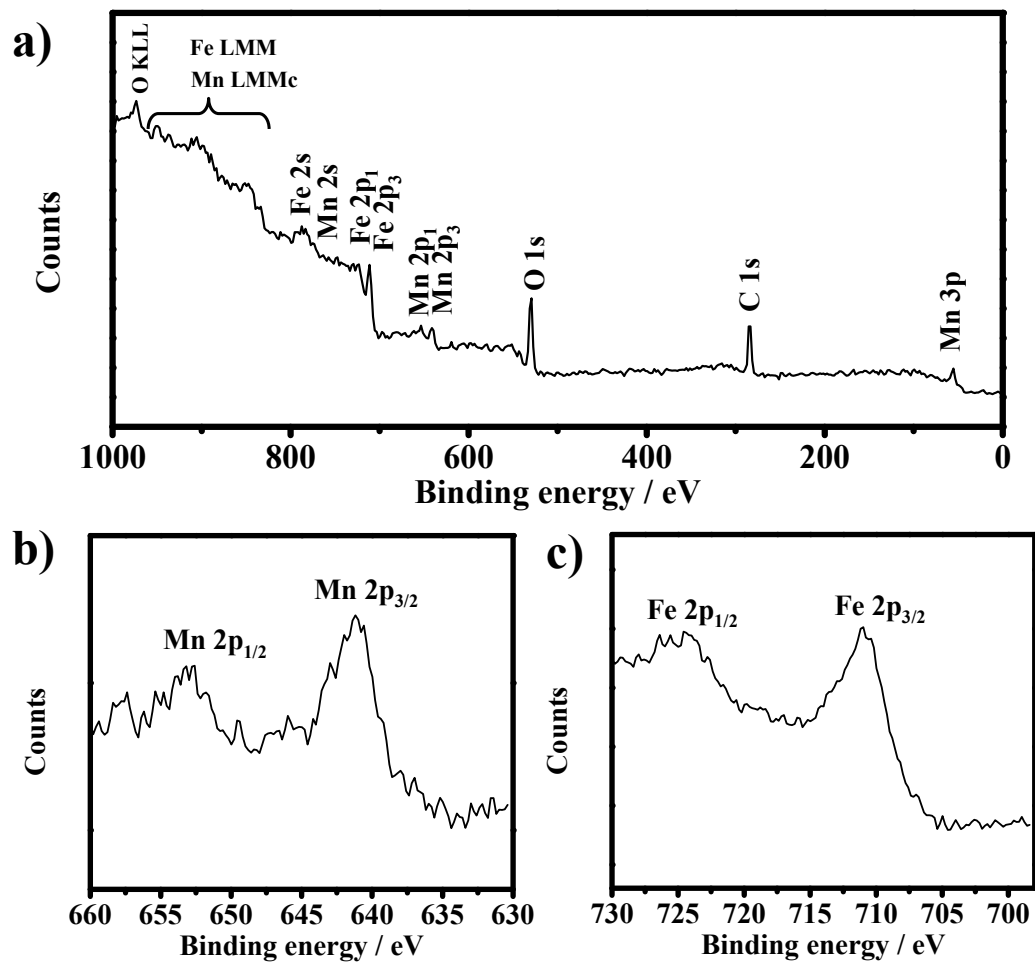


**Figure S1.** a) XPS spectrum and high-resolution core-level spectra of b) Mn 2p and c) Fe 2p for core-shell nanocubes.

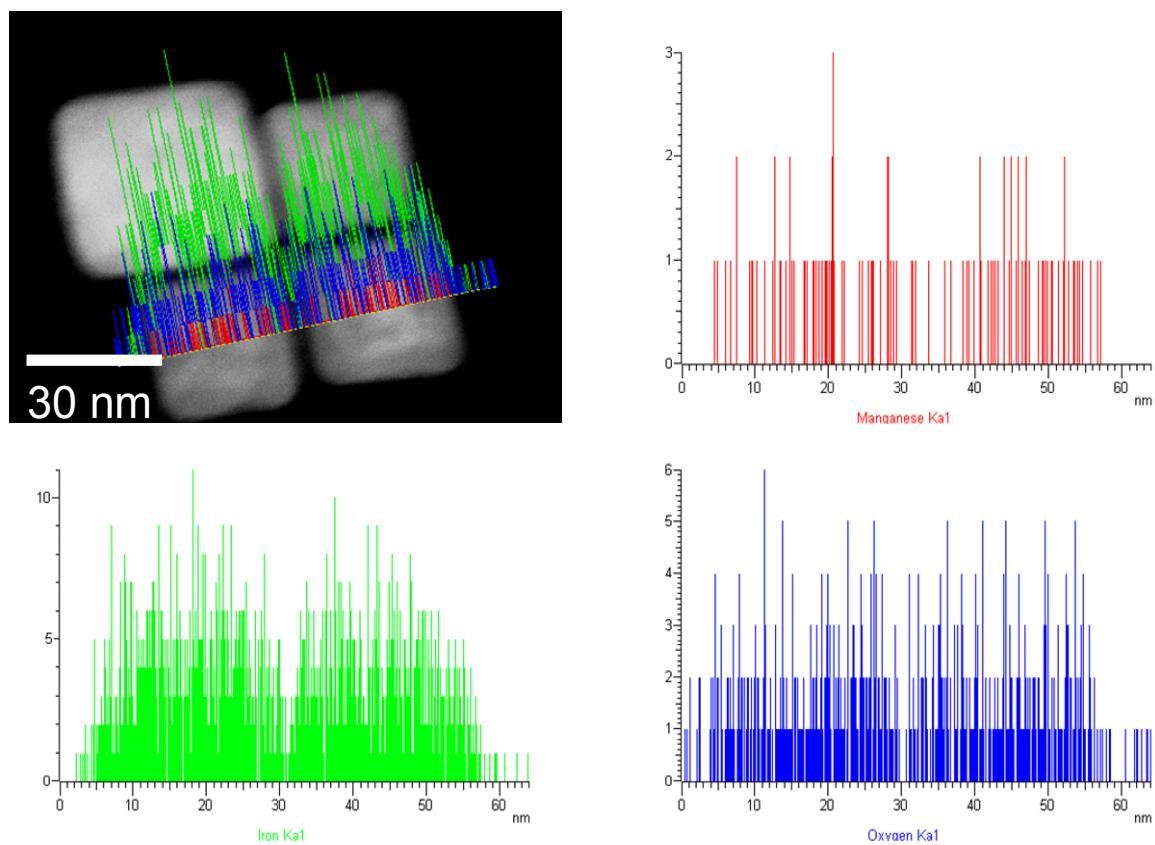


**Figure S2.** HAADF STEM image with corresponding line-scan EDS profiles of two core-shell nanostructures using  $\text{Mn}(\text{ac})_2$  and  $\text{Fe}(\text{acac})_3$  reactants via a two-step reaction process after heating to  $290\text{ }^\circ\text{C}$  (process i in Scheme 1a). The red, green, and blue signals respectively indicate the distributions of Mn, Fe, and O elements.

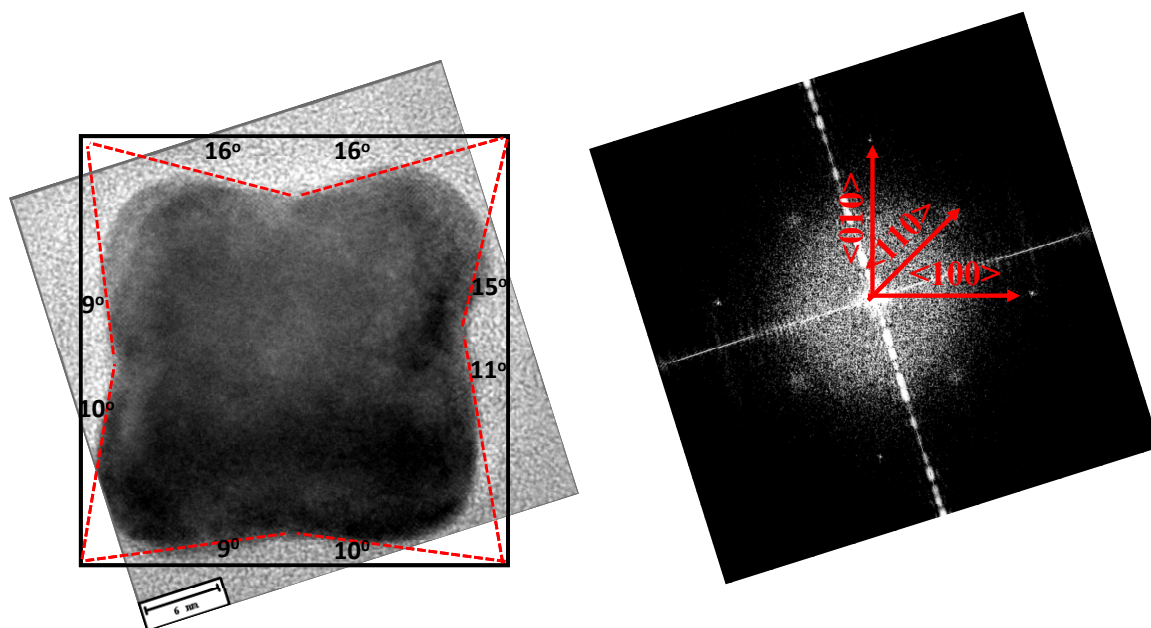


**Figure S3.** HRTEM image of a NaCl-type nanocube (left) and the corresponding fast Fourier transform (FFT) analysis (right). The angles between the facets of the [001]-projected nanocube and the {100} facets of an ideal cube were determined as 16°, 16°, 15°, 11°, 10°, 10°, 10°, 9°, which respectively correspond to the {720}, {720}, {720}, {510}, {510}, {510}, {510}, {510} facets. The black square in the HRTEM image represents an ideal cube.

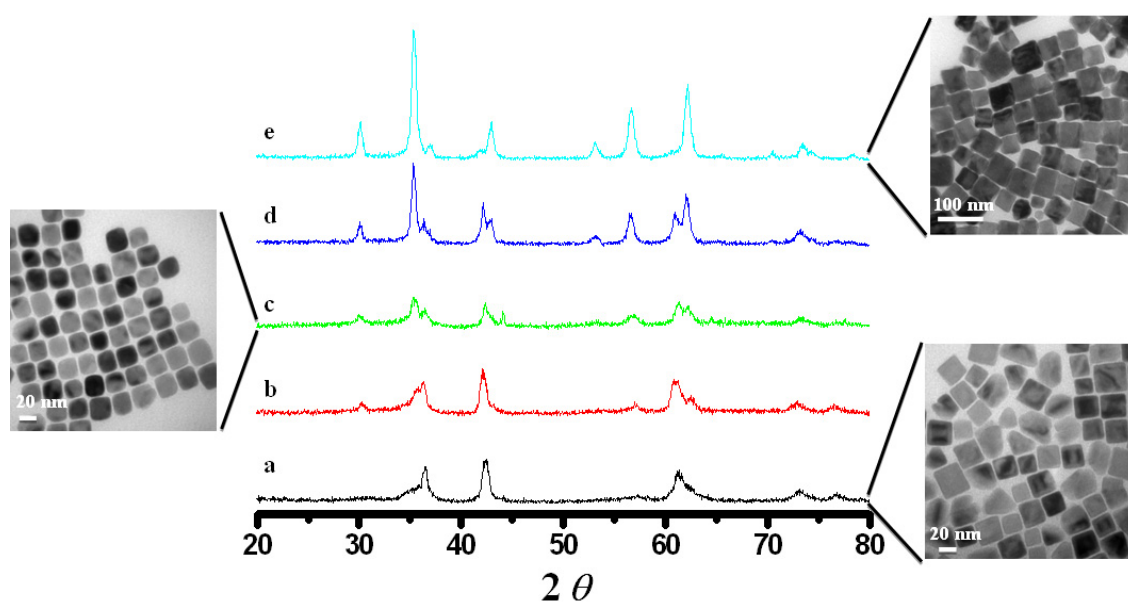


**Figure S4.** XRD measurements of the core-shell nanocubes as a function of aging period at 290°C in air (process ii in Scheme 1a): a) 0 min, b) 25 min, c) 40 min, d) 60 min, and e) 150 min. The TEM images show the nanocubes corresponding to the products of XRD patterns at a (0 min), c (40 min), and e (150 min).

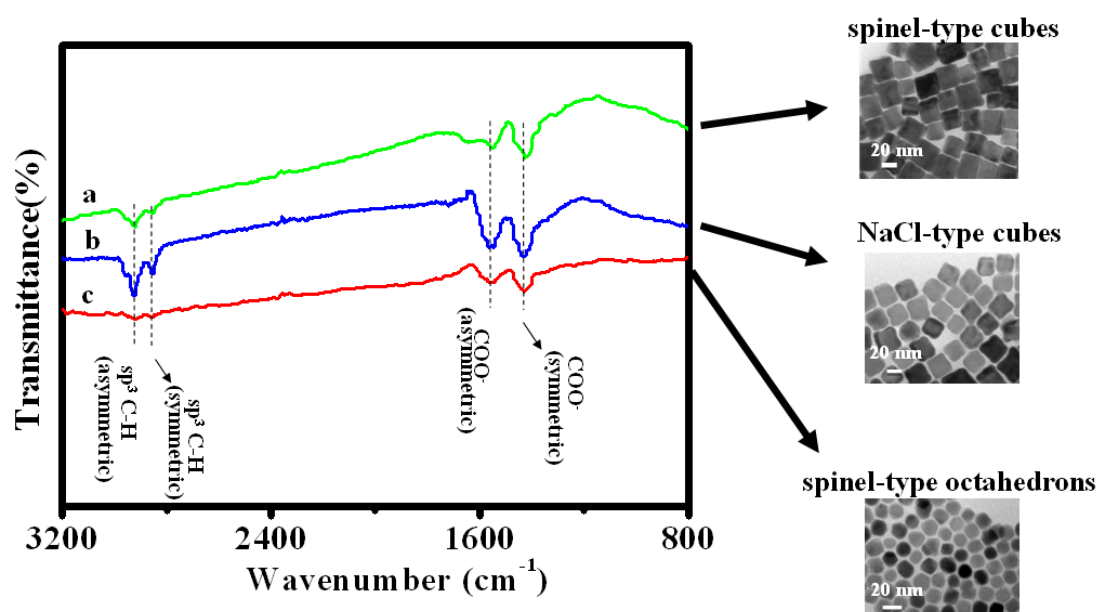


**Figure S5.** FT-IR spectra of a) spinel-type nanocubes, b) NaCl-type nanocubes, and c) spinel-type nano-octahedrons. The absorption bands, including  $\sim 1550\text{ cm}^{-1}$ , and  $\sim 1424\text{ cm}^{-1}$ , correspond to asymmetric and symmetric COO<sup>-</sup> vibrations originating from oleic acid.<sup>1</sup>

1. Guilherme V. M. Jacintho, Alexandre G. Brolo, Paola Corio, Paulo A. Z. Suarez, and Joel C. Rubim *J. Phys. Chem. C* **7684** **2009**, *113*, 7684.

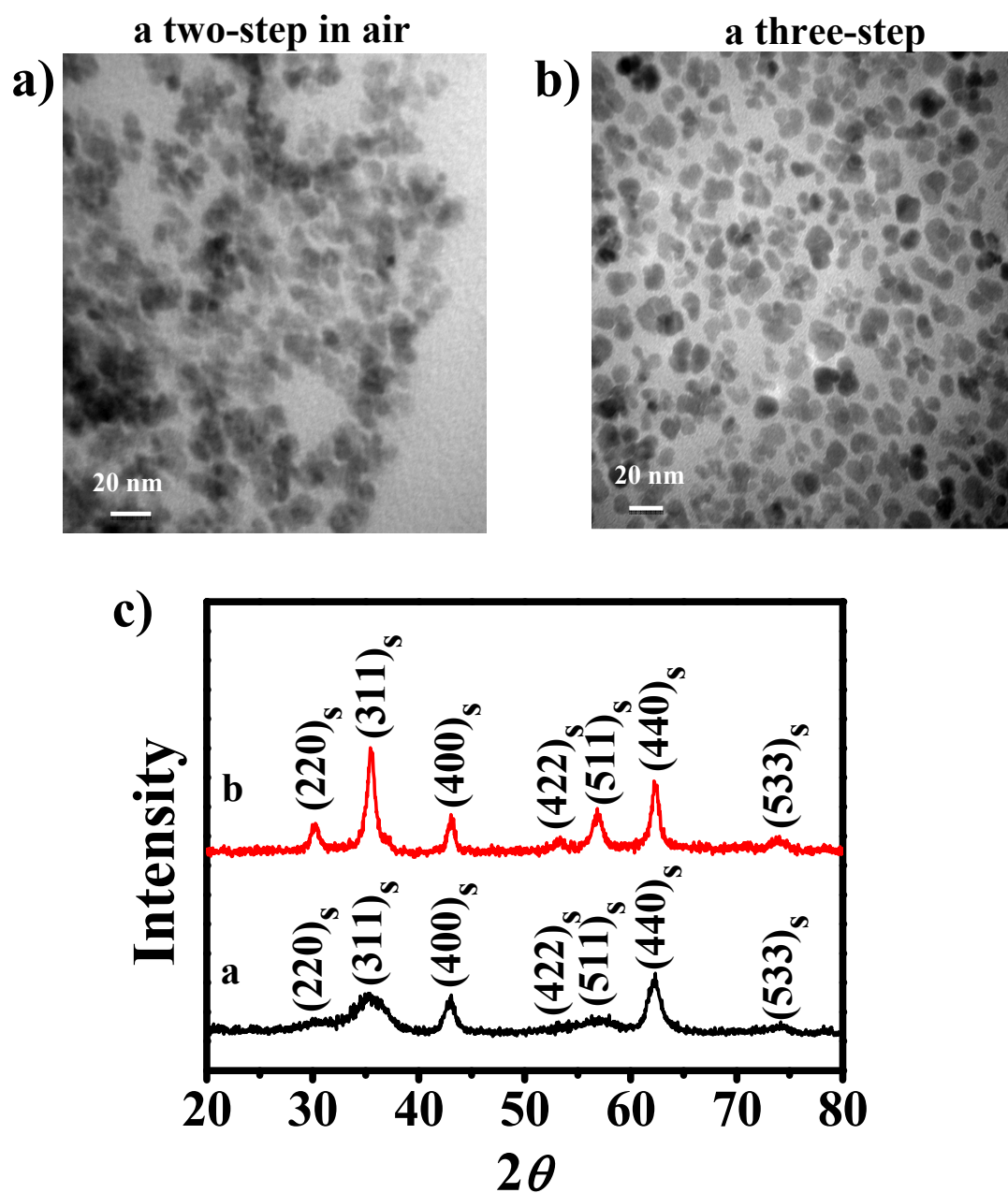


**Figure S6.** TEM images of a) oleic acid decreased to 1 mL leading to a spinel structure after heating to 290 °C at heating rate of 11.5 °C/min, the reaction corresponding to process i in Scheme 1a; b) oleic acid decreased to 1 mL resulting in a spinel structure by following a three-step process after going through the consecutive processes iv, v, and vi in Scheme 1b. c) XRD reveals spinel structures corresponding to a) and b) products of TEM images. The subscript s indicates a spinel crystal structure.

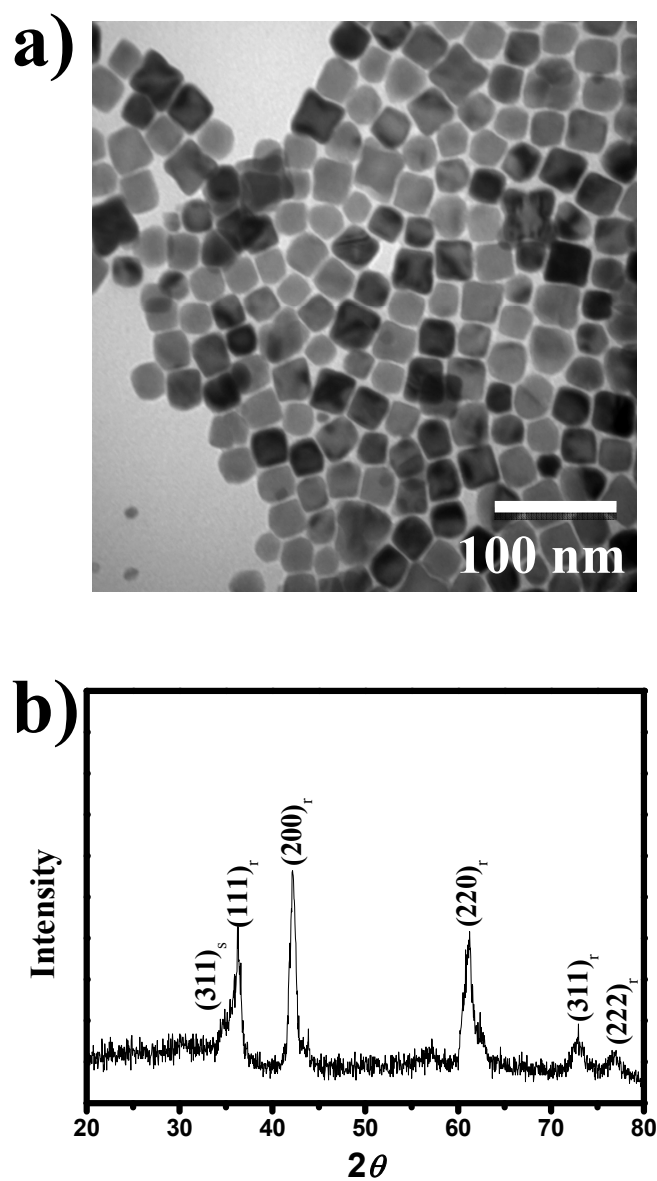


**Figure S7.** a) TEM image and b) XRD pattern determined from the collected nanocube products when the oleic acid was increased to 8.36 mL following a two-step heating process (process i and ii of Scheme 1a) with a heating rate of 11.5 °C/min to 290 °C in air (i), followed by heating at 290 °C for 1 h in air (ii). The subscripts r and s respectively represent NaCl-type (rock-salt) and spinel-type structures.

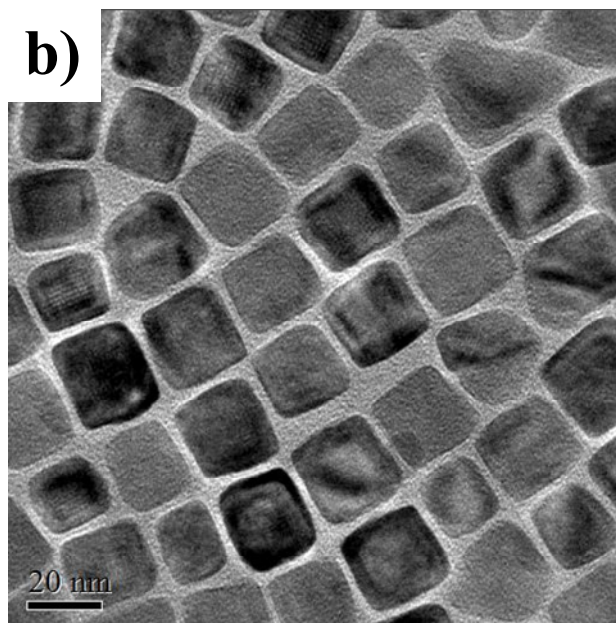
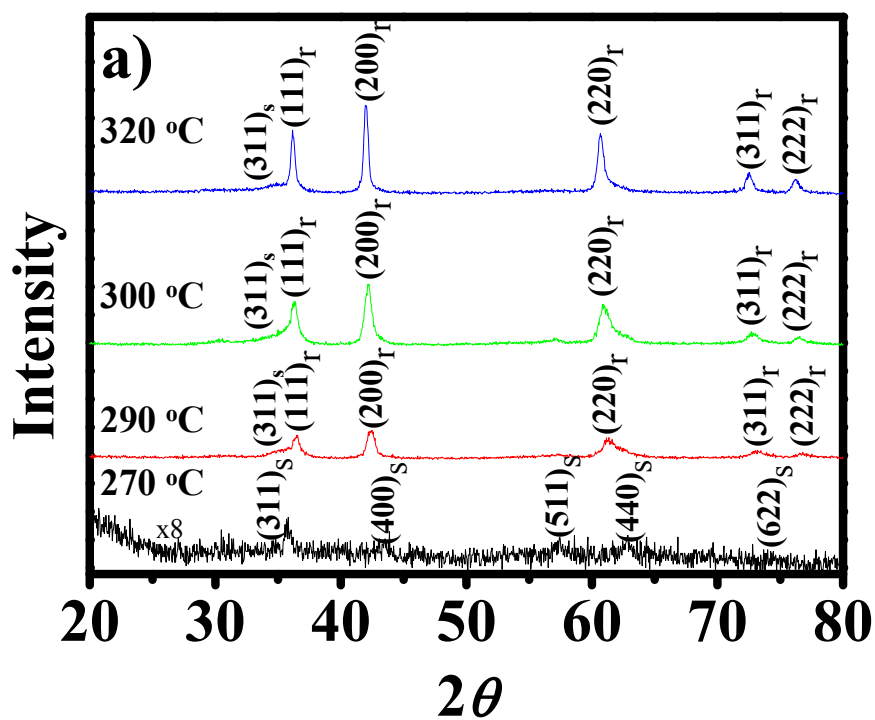


**Figure S8.** a) XRD evolution as a function of heating temperature. b) TEM image corresponding to annealing at 300 °C (process i in Scheme 1a). The subscripts r and s respectively represent NaCl-type (rock-salt) and spinel-type structures.

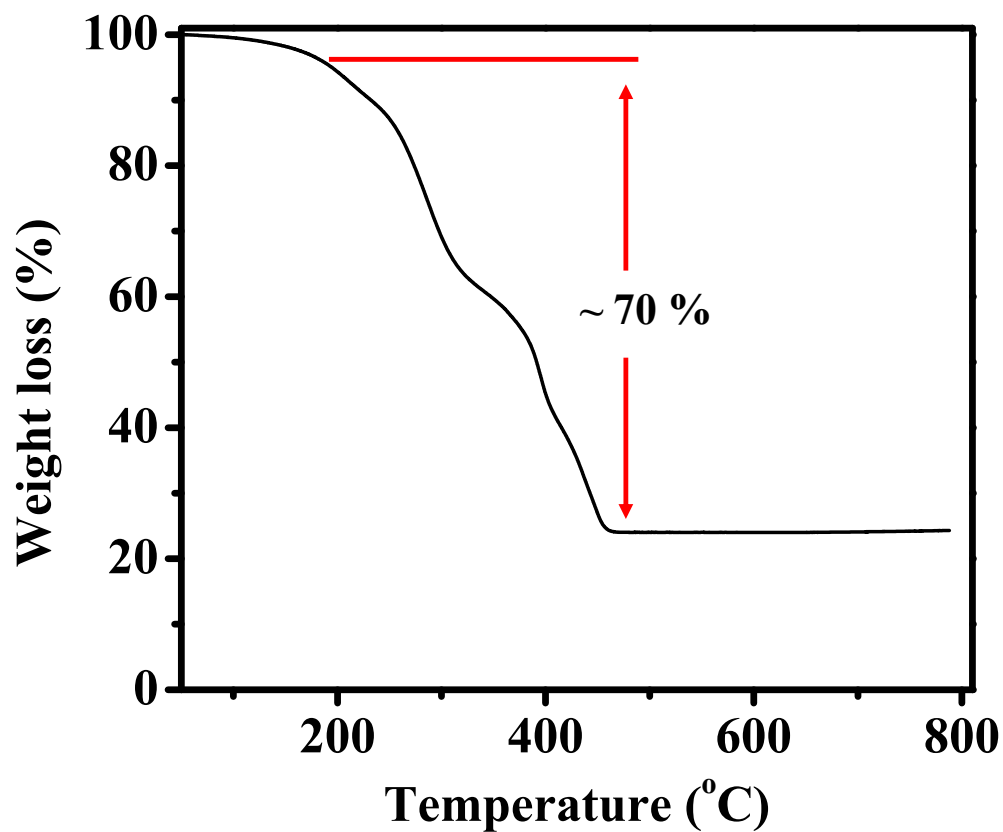


**Figure S9.** TGA measurement of nanocrystals collected at 270 °C from the process iv in Scheme 1b. The initial weight loss of 6% below 200 °C is due to the loss of adsorbed solvent, while a loss of weight of ~ 70 % above 200 °C is attributed to the elimination of organic contaminants.

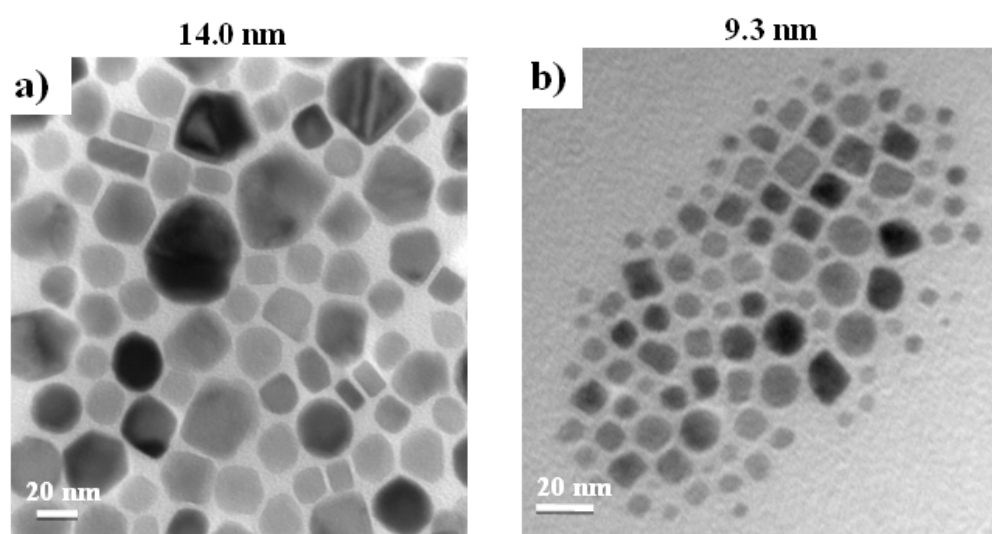


**Figure S10.** TEM evolution as a function of aging period for process v in Scheme 1b: at a) 15 min and b) 30 min.

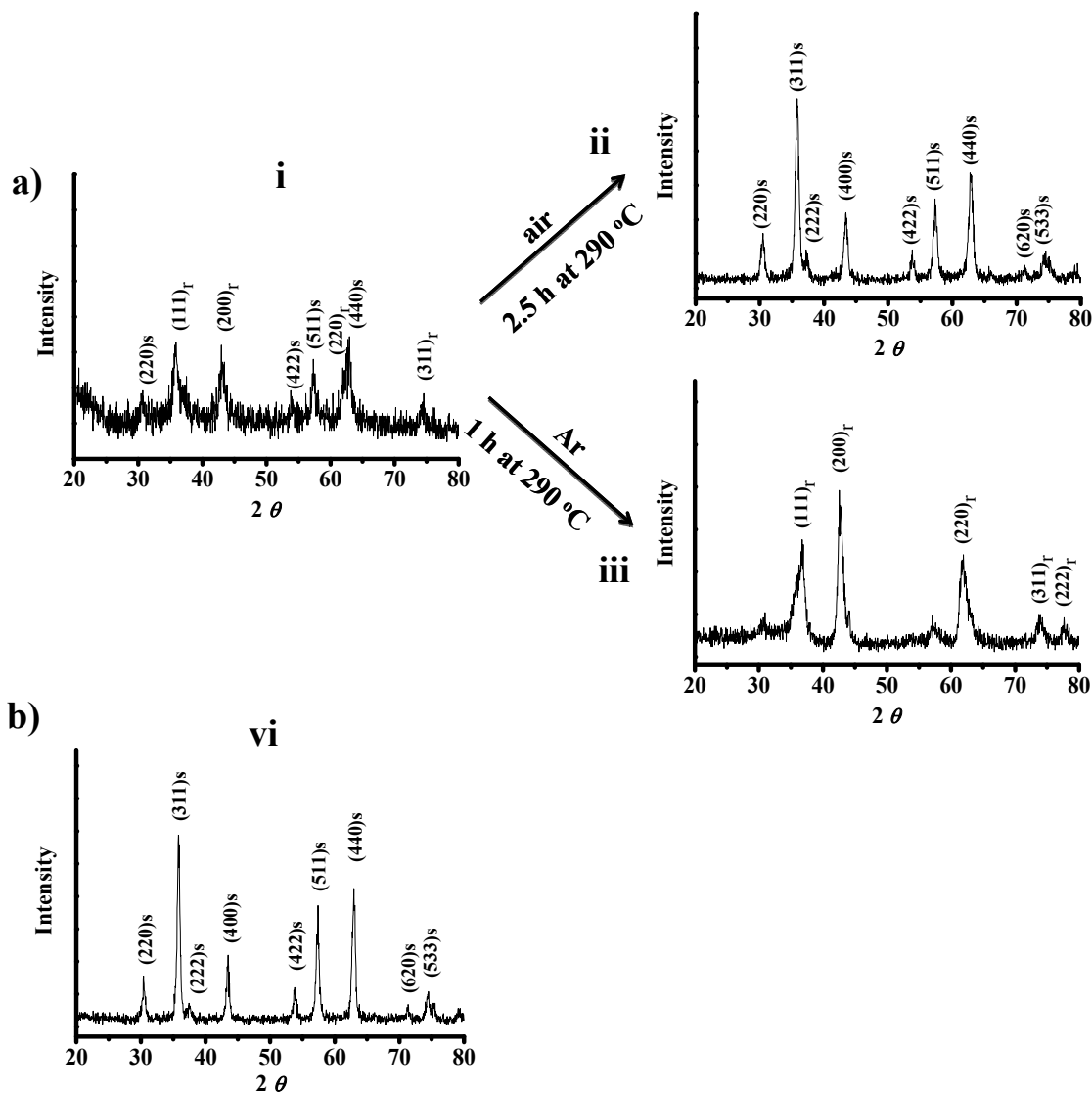


**Figure S11.** XRD patterns of the ternary M-Fe-O nanocubes using  $\text{Co}(\text{ac})_2$  and  $\text{Fe}(\text{acac})_3$  reactants following a) a two-step reaction process in Scheme 1a through processes i→ii or i→iii and b) a three-step heating process in Scheme 1b through a processes iv-v-vi. The subscripts r and s respectively represent NaCl-type (rock-salt) and spinel-type structures.

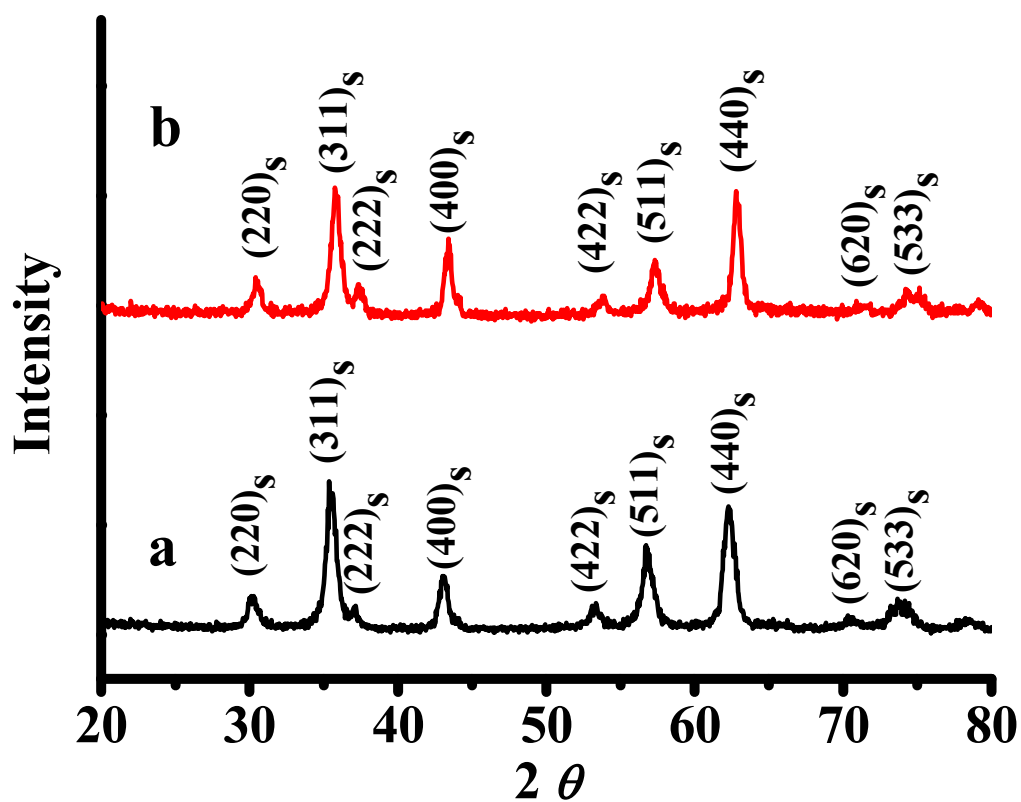


**Figure S12.** XRD patterns of the ternary M-Fe-O nanocubes using M(acac)<sub>2</sub> and Fe(acac)<sub>3</sub> reactants following a two-step reaction process through consecutive processes i and ii in Scheme 1a, where M: a) Mn and b) Co. The subscript s represents spinel-type structure.

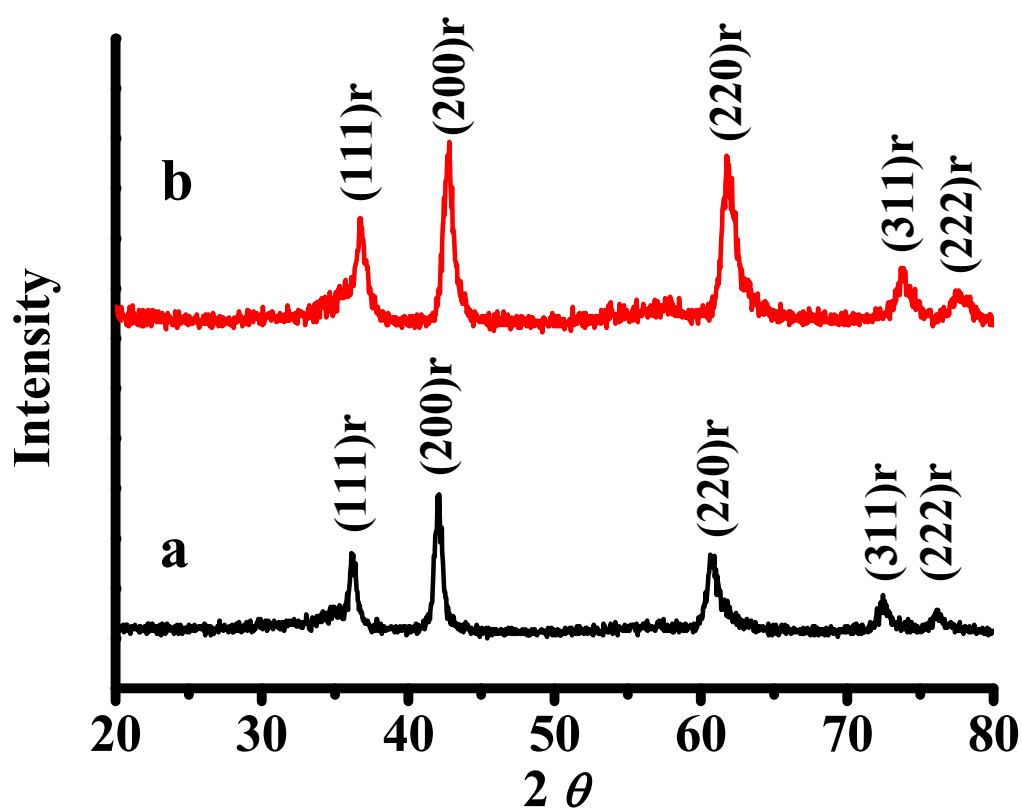


**Figure S13.** XRD patterns of the ternary M-Fe-O nanocubes using  $M(\text{acac})_2$  and  $\text{Fe}(\text{acac})_3$  reactants following a two-step reaction process through consecutive processes i and iii in Scheme 1a, where M: a) Mn and b) Co. The subscript r represents NaCl-type (rock-salt) structure.

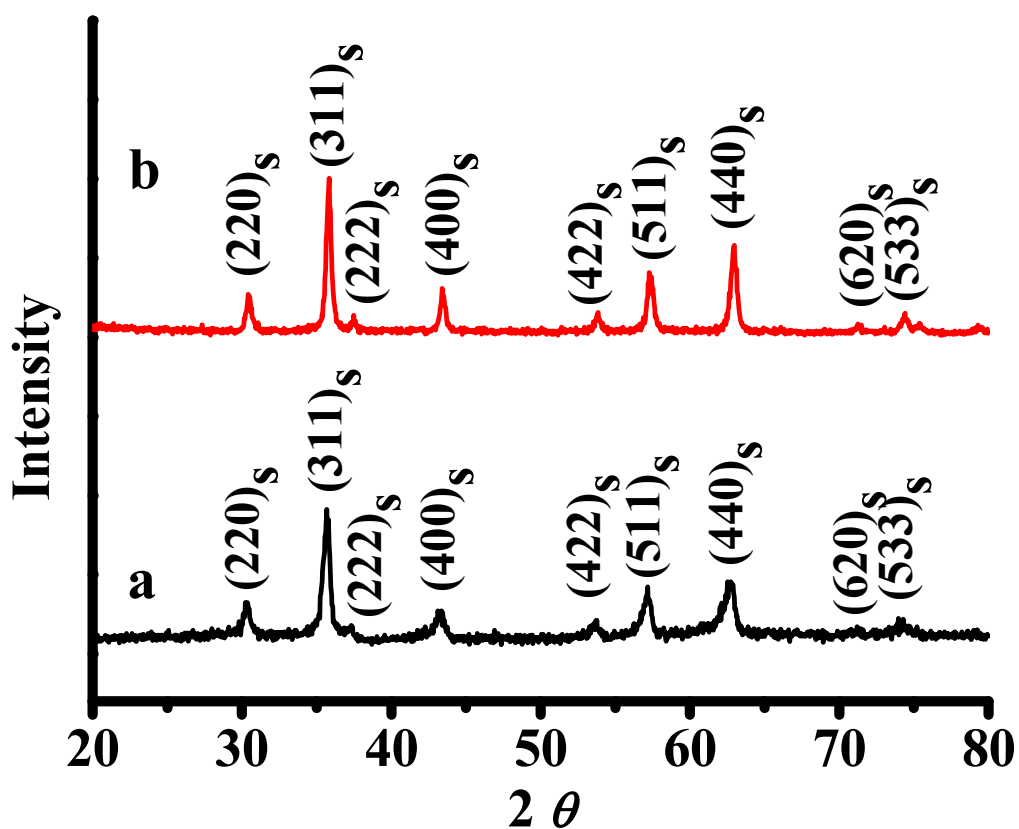


**Figure S14.** XRD patterns of the spinel M-Fe-O nanooctahedrons from a three-step heating process through consecutive processes iv, v, and vi in Scheme 1b, where M: a) Mn and b) Co. The subscript s represents spinel crystal structure.